The Plant Cell, Vol. 20: 888–900, April 2008, www.plantcell.org © 2008 American Society of Plant Biologists

Interaction of *KNAT6* and *KNAT2* with *BREVIPEDICELLUS* and *PENNYWISE* in *Arabidopsis* Inflorescences [W]

Laura Ragni, Enric Belles-Boix, Markus Günl,[1] and Véronique Pautot[2]

Laboratoire de Biologie Cellulaire, Institut Jean-Pierre Bourgin, Institut National de la Recherche Agronomique, 78026 Versailles Cedex, France

The three amino acid loop extension (TALE) homeodomain superfamily, which comprises the KNOTTED-like and BEL1-like families, plays a critical role in regulating meristem activity. We previously demonstrated a function for *KNAT6* (for *KNOTTED*-like from *Arabidopsis thaliana 6*) in shoot apical meristem and boundary maintenance during embryogenesis. *KNAT2*, the gene most closely related to *KNAT6*, does not play such a role. To investigate the contribution of *KNAT6* and *KNAT2* to inflorescence development, we examined their interactions with two *TALE* genes that regulate internode patterning, *BREVIPEDICELLUS* (*BP*) and *PENNYWISE* (*PNY*). Our data revealed distinct and overlapping interactions of *KNAT6* and *KNAT2* during inflorescence development. Removal of KNAT6 activity suppressed the *pny* phenotype and partially rescued the *bp* phenotype. Removal of KNAT2 activity had an effect only in the absence of both *BP* and *KNAT6* or in the absence of both *BP* and *PNY*. Consistent with this, *KNAT6* and *KNAT2* expression patterns were enlarged in both *bp* and *pny* mutants. Thus, the defects seen in *pny* and *bp* are attributable mainly to the misexpression of *KNAT6* and to a lesser extent of *KNAT2.* Hence, our data showed that BP and PNY restrict *KNAT6* and *KNAT2* expression to promote correct inflorescence development. This interaction was also revealed in the carpel.

INTRODUCTION

The aerial part of the plant results from the activity of the shoot apical meristem (SAM). The SAM has two main functions: the maintenance of a population of stem cells and the production of organs. In *Arabidopsis thaliana*, the three amino acid loop extension (TALE) homeodomain superfamily plays a critical role in determining meristem function (for review, see Ragni et al., 2007). This family comprises the *KNAT* (for *KNOTTED*-like from *Arabidopsis thaliana*) members and the *BEL1*-like (*BELL*) members that can form heterodimers to regulate plant development. *KNAT* class I contains four members: *SHOOT MERISTEMLESS* (*STM*), *BREVIPEDICELLUS* (*BP*)/*KNAT1*, *KNAT2*, and *KNAT6. STM* is required for the initiation of the meristem during embryogenesis and its maintenance during postembryonic development (Clark et al., 1996; Endrizzi et al., 1996; Long et al., 1996). *BP* contributes with *STM* to SAM maintenance since the loss of function of *BP* reduces the residual meristematic activity of the weak allele *stm-2* (Byrne et al., 2002, 2003). Like *BP*, *KNAT6* contributes redundantly with *STM* to SAM function, as the inactivation of *KNAT6* abolishes the meristematic potential of the weak allele *stm-2* (Belles-Boix et al., 2006). In addition, a specific role for *KNAT6* in boundary maintenance is indicated by a severe defect in cotyledon separation observed in the *stm-2 knat6* double mutant (Belles-Boix et al., 2006). *KNAT2* also is expressed in the SAM, but its role is unclear as its inactivation does not aggravate *stm-2*, *knat6 stm-2*, or *knat6 bp stm-2* phenotypes (Belles-Boix et al., 2006). *PENNYWISE* (*PNY*), a member of the *BELL* family, also known as *BELLRINGER*, *REPLUMLESS* (*RPL*), or *VAAMANA*, contributes to SAM maintenance redundantly with *STM* (Byrne et al., 2003).

In addition to their contributions to SAM function, *BP* and *PNY* regulate inflorescence development. *BP* plays a primary role in inflorescence growth, as indicated by *bp* mutants that exhibit reduced internode and pedicel lengths, bends at nodes, and downward-oriented siliques (Douglas et al., 2002; Venglat et al., 2002; Smith and Hake, 2003). *PNY* influences inflorescence architecture and fruit development (Byrne et al., 2003; Smith and Hake, 2003; Bhatt et al., 2004). PNY also interacts with BP to regulate inflorescence patterning and fruit development (Smith and Hake, 2003; Alonso-Cantabrana et al., 2007). A role for *STM* in inflorescence growth also is suggested as weak alleles of *STM* show aberrant organ position, fusion defects, and abnormal flowers (Endrizzi et al., 1996; Kanrar et al., 2006). However, these defects may be indirect effects resulting from the abnormal structure of the SAM. *KNAT2* and *KNAT6* are the most closely related members of class I; however, *knat2*, *knat6*, and *knat2 knat6* mutants show wild-type development (Belles-Boix et al., 2006). Here, we investigated the genetic interaction of *KNAT6* and *KNAT2* with *BP* and *PNY* during inflorescence development. Our studies show that in wild-type plants, *PNY* and *BP* restrict *KNAT6* and *KNAT2* expression to promote correct inflorescence growth.

[1] Current address: Michigan State University–Department of Energy Plant Research Laboratory, Michigan State University, East Lansing, MI 48824-1312.

[2] Address correspondence to pautot@versailles.inra.fr.

The author responsible for distribution of materials integral to the findings presented in this article in accordance with the policy described in the Instructions for Authors (www.plantcell.org) is: Véronique Pautot (pautot@versailles.inra.fr).

[W] Online version contains Web-only data.

www.plantcell.org/cgi/doi/10.1105/tpc.108.058230

RESULTS

The Inactivation of *KNAT6* Partially Rescues the *bp* Phenotype

To analyze the interaction of *KNAT6* and *KNAT2* with *BP*, we generated the *knat6 bp*, *knat2 bp*, and *knat2 knat6 bp* mutants. *bp* mutants are characterized by reduced stature, partial loss of apical dominance, and downward-oriented siliques (Douglas et al., 2002; Venglat et al., 2002; Smith and Hake, 2003). Figure 1 shows the phenotypes of the main inflorescences of the *bp*, *knat2 bp*, *knat6 bp*, and *knat2 knat6 bp* mutants. The inactivation of *KNAT2* alone did not alter the *bp* phenotype, whereas the inactivation of *KNAT6* partially rescued it (Figures 1C and 1D). The downward orientation of siliques in *bp* mutants was partially rescued in *knat6 bp* double mutants and was completely rescued in the absence of both *KNAT6* and *KNAT2* (Figures 1D, 1E, and 2D). We performed quantitative phenotypic analyses on 10 plants of each genotype to further characterize the double and triple mutants. The height of the plants, the number of rosette paraclades, and the internode size between siliques along the main inflorescence were determined. These measurements first were performed on the *knat2* and *knat6* single mutants and on the *knat2 knat6* double mutant and confirmed that these mutants exhibit essentially wild-type development with respect to these features (Belles-Boix et al., 2006; see Supplemental Figures 1 and 2 online). The same analyses were then performed on *bp*, *knat2 bp*, *knat6 bp*, and *knat2 knat6 bp* mutants. The average heights of the *bp* and *knat2 bp* mutants were 21 cm shorter, and those of *knat6 bp* and *knat6 knat2 bp* were 7 cm shorter than that of the wild type (Figure 2A). The *bp* mutants showed a partial loss of apical dominance as they produced six to eight rosette paraclades, whereas wild-type plants produced three to five paraclades on average (Figure 2B). This defect was rescued in the *knat6 bp* and *knat6 knat2 bp* mutants but not in the *knat2 bp* mutants (Figure 2B). We then examined the distribution of siliques along the main inflorescence. The *bp* mutants showed short internodes as 75% of *bp* internodes ranged in length from 0 to 5 mm, whereas 74% of wild-type internodes ranged in length from 6 to 15 mm (Figure 2C). The distribution of internode length along the main inflorescence of the *knat2 bp* double mutants was similar to that of *bp* (Figure 2C). By contrast, an increase of internode length was observed in the *knat6 bp* and *knat6 knat2 bp* mutants, since 50% of internodes ranged in length from 6 to 15 mm in both genotypes (Figure 2C). Thus, the inactivation of *KNAT6* partially rescued the *bp* phenotypic features; by contrast, the inactivation of *KNAT2* did not show such an effect. However, a redundant role of *KNAT2* with *KNAT6* in silique orientation was revealed (Figure 2D).

KNAT6 and *KNAT2* Expression Domains Are Enlarged in the *bp* Mutant

Since we observed that *bp* defects were partially rescued in the *knat6 bp* and *knat2 knat6 bp* mutants, we examined the expression patterns of *KNAT2* and *KNAT6* in *bp* mutants. The expression patterns of *PKNAT6-GUS* (for β-glucuronidase) and *PKNAT2:GUS* fusions were analyzed in the *bp-9* background. In wild-type inflorescences, *KNAT6* and *KNAT2* expression overlapped partially. Both KNAT6-GUS and KNAT2-GUS activities were detected in the floral pedicel axils (Figures 3A and 4A). In floral buds, KNAT6-GUS was restricted to the boundaries between floral organs, whereas KNAT2-GUS was expressed at the base of the floral meristem (Figures 3E and 4E). By contrast, in the *bp* inflorescences, the domains of *KNAT6* and *KNAT2* expression were enlarged, although their patterns were distinct. In *bp* mutants, an ectopic KNAT6-GUS activity was present in the main stem and in young pedicels, whereas an ectopic KNAT2-GUS activity was detected only in the pedicels (Figures 3B, 3F, 4B, and 4F). Thus, in wild-type inflorescences, BP restricted

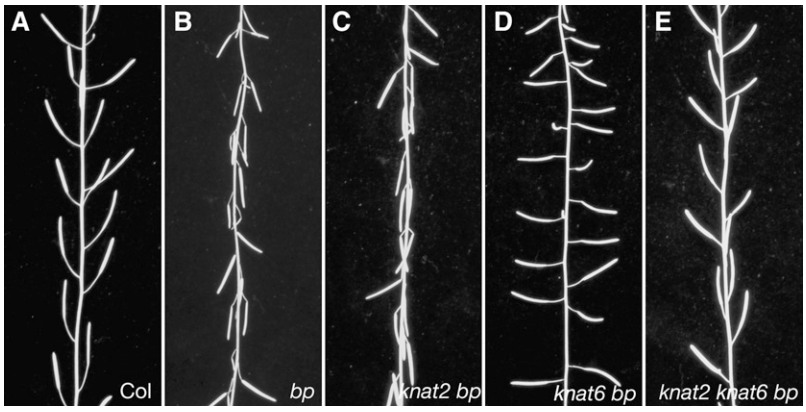

Figure 1. Phenotype of the *knat2 bp*, *knat6 bp*, and *knat2 knat6 bp* Mutants.

(A) Wild-type inflorescence.
(B) *bp* inflorescence with downward oriented siliques.
(C) *knat2 bp* inflorescence. The inactivation of *KNAT2* did not alter the *bp* phenotype.
(D) *knat6 bp* inflorescence. The inactivation of *KNAT6* partially rescued the *bp* phenotype.
(E) *knat2 knat6 bp* inflorescence. The orientation of the siliques was wild type in the *knat2 knat6 bp* triple mutant.

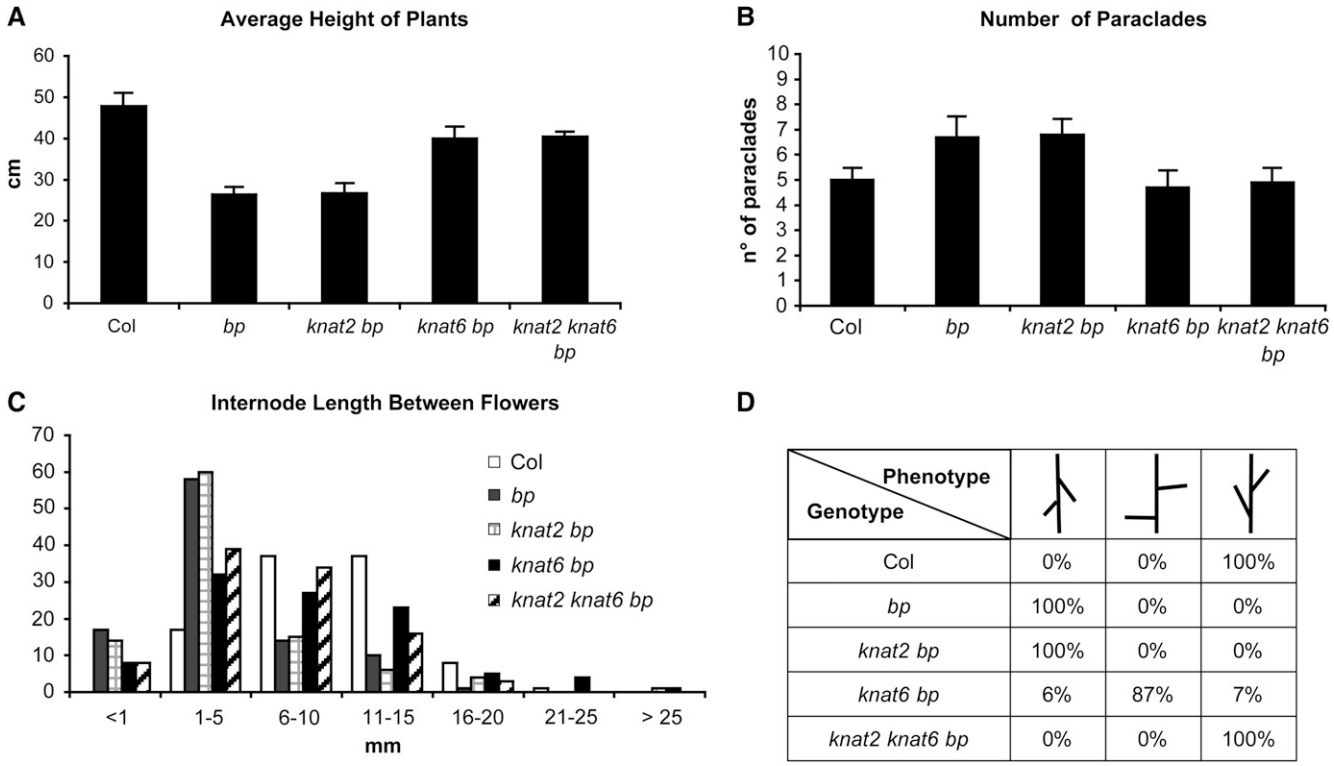

Genotype \ Phenotype			
Col	0%	0%	100%
bp	100%	0%	0%
knat2 bp	100%	0%	0%
knat6 bp	6%	87%	7%
knat2 knat6 bp	0%	0%	100%

Figure 2. Quantitative Phenotypic Analyses of the *knat2 bp*, *knat6 bp*, and *knat2 knat6 bp* Mutants.

Ten plants for each genotype were analyzed.
(A) Average (+SD) height of wild-type, *bp*, *knat2 bp*, *knat6 bp*, and *knat2 knat6 bp* plants. The inactivation of *KNAT6* partially rescued the defect in size of *bp*.
(B) Average (+SD) number of rosette paraclades of wild-type, *bp*, *knat2 bp*, *knat6 bp*, and *knat2 knat6 bp* plants.
(C) Distribution of the length of the internode between two successive siliques. Ten internodes between the 1st and 11th siliques (counting acropetally) were measured.
(D) Orientation of the pedicels in the wild type, *bp*, *knat2 bp*, *knat6 bp*, and *knat2 knat6 bp*.

KNAT6 expression in pedicels and stem and *KNAT2* expression in pedicels.

The Inactivation of *KNAT6* Rescues the *pny* Phenotype

Since *BP* and *PNY* cooperate to regulate inflorescence development (Smith and Hake, 2003), we examined the interaction of *KNAT2* and *KNAT6* with *PNY*. *pny* mutants are characterized by phyllotaxy defects, partial loss of apical dominance, and reduced stature (Byrne et al., 2003; Roeder et al., 2003; Smith and Hake, 2003; Bhatt et al., 2004). In addition, the *pny* mutant shows fruit alterations, such as defects in replum differentiation and in septum fusion (Byrne et al., 2003; Roeder et al., 2003). To investigate the interaction between *KNAT2*, *KNAT6*, and *PNY*, we generated the *knat2 pny*, *knat6 pny*, and *knat2 knat6 pny* mutants. The *knat2 pny* double mutants showed a *pny* phenotype (Figures 5 and 6; see Supplemental Figure 3 online) and confirmed previous data (Byrne et al., 2003). Surprisingly, the *knat6 pny* double mutant showed a wild-type phenotype (Figure 5D). The same phenotype was obtained using both alleles of *KNAT6* (data not shown). The distribution of organs along inflorescences in the *knat6 pny* double mutant was the same as in the wild type. Moreover, the average height of the *knat6 pny* double mutant plants was the same as that of the wild type, whereas the *pny* mutant plants were 10 cm shorter on average than the wild type (Figure 6A). The partial loss of apical dominance seen in the *pny* mutants was rescued in the *knat6 pny* double mutant (Figure 6B). Whereas *pny* produced five to eight rosette paraclades, the *knat6 pny* double mutants produced four to five paraclades. In addition, the distribution of the internode lengths between flowers was comparable in the wild type and in the *knat6 pny* double mutant (Figure 6C). The *pny* mutants were characterized by internodes with irregular lengths, being shorter than 6 mm in 38% of the internodes, and longer than 25 mm in 15% of the internodes. By contrast, 63 and 60% of the internodes ranged in length from 6 to 15 mm in inflorescences from the *knat6 pny* double mutant and the wild type, respectively.

To further describe the internode patterning in the *knat6 pny* double mutant, we measured the phyllotactic pattern using the device and the method described previously (Peaucelle et al., 2007). The divergence angle between the insertion points of two successive floral pedicels along the main inflorescence was determined. Fifteen divergence angles between the 1st and 16th siliques (counting acropetally) of each inflorescence were

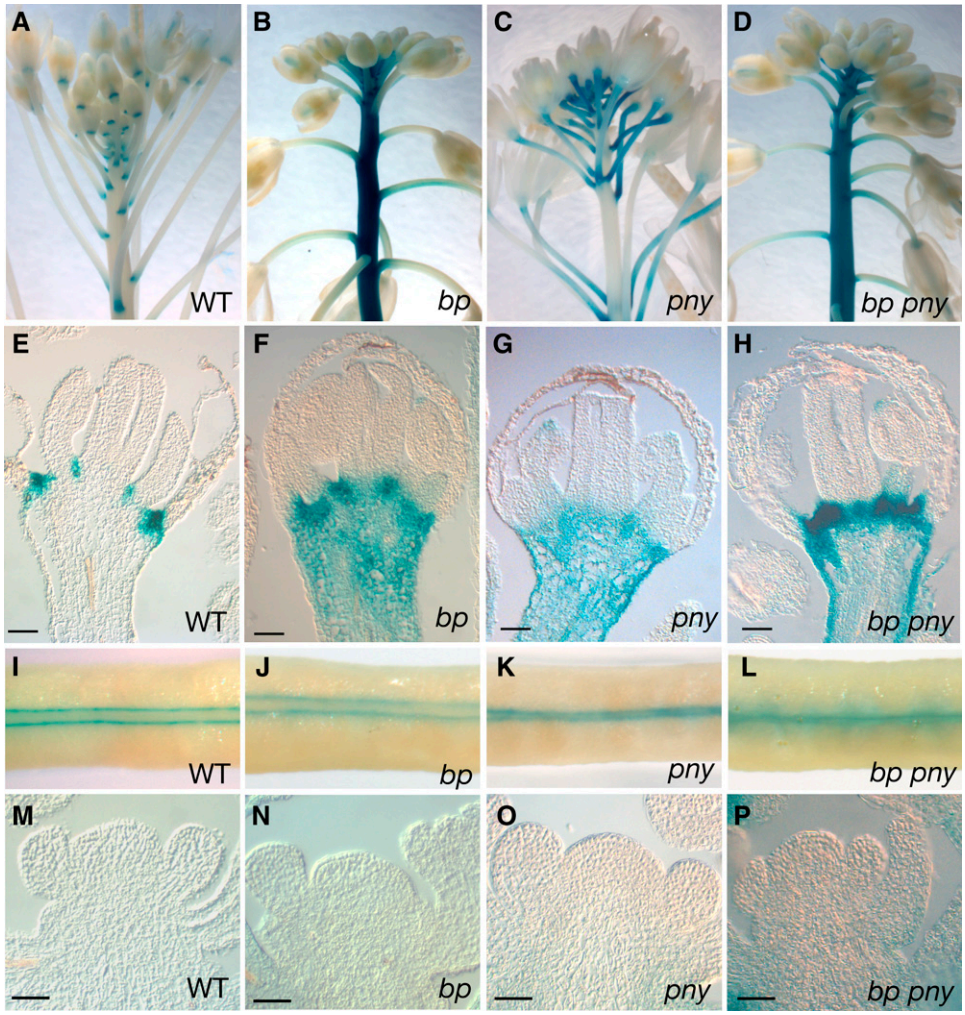

Figure 3. KNAT6-GUS Expression in *bp*, *pny*, and *bp pny* Mutants.

(A) Wild-type inflorescence showing GUS activity in the axil and in the distal part of the pedicel.
(B) *bp* inflorescence showing GUS activity in the main stem and in the pedicels.
(C) *pny* inflorescence showing GUS activity in the pedicels.
(D) *bp pny* inflorescence showing GUS activity in the main stem and in the pedicels.
(E) Median longitudinal section through a wild-type stage 12 flower showing GUS activity restricted to the boundaries between floral organs (bar = 40 μm).
(F) Median longitudinal section through a *bp* stage 12 flower showing GUS activity in the pedicel (bar = 40 μm).
(G) Median longitudinal section through a *pny* stage 12 flower showing GUS activity in the pedicel (bar = 40 μm).
(H) Median longitudinal section through a *bp pny* stage 12 flower showing GUS activity in the pedicel (bar = 40 μm).
(I) Wild-type carpel showing GUS activity in boundaries between the valves and the replum.
(J) *bp* carpel showing GUS activity in valves margins.
(K) *pny* carpel showing GUS activity between the valves. The *pny* carpel has a narrower replum.
(L) *bp pny* carpel showing GUS activity between the valves.
(M) Longitudinal median section through a wild-type inflorescence meristem showing no GUS activity (bar = 40 μm).
(N) *bp* inflorescence meristem with no GUS activity (bar = 40 μm).
(O) *pny* inflorescence meristem with no GUS activity (bar = 40 μm).
(P) *bp pny* inflorescence meristem with no GUS activity (bar = 40 μm).

measured according to the orientation of the generative spiral. In wild-type Columbia (Col) ecotype, the mean divergence angle was 143° ($n = 150$). Only 39% of the divergence angles fell within the range from 120 to 149, which contains the theoretical angle of 137.5° (Figure 7A). This proportion increased to 80% if the class was enlarged to encompass angles ranging from 90° to 179°. The value of the mean divergence angle was higher than the theoretical value and more variable. This was consistent with the recent observation showing that the phyllotactic pattern in *Arabidopsis* is less robust during reproductive development

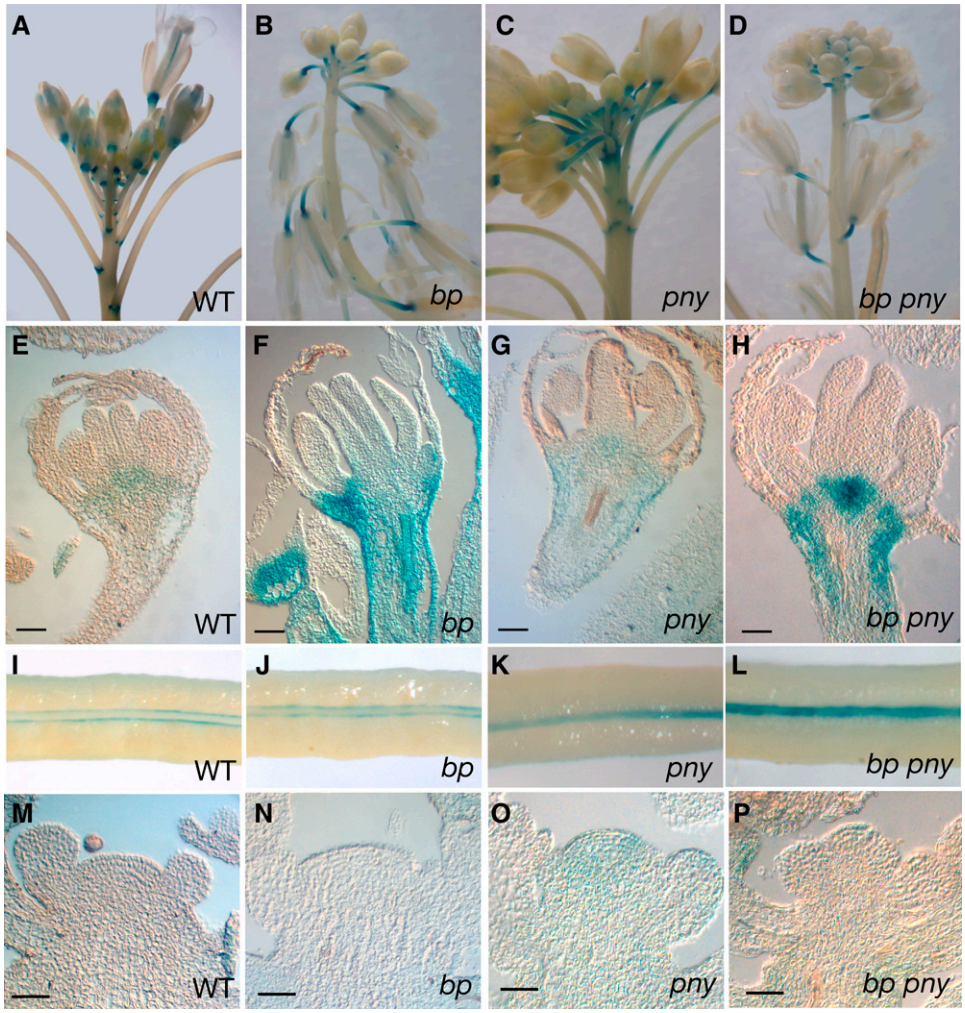

Figure 4. KNAT2-GUS Expression in *bp*, *pny*, and *bp pny* Mutants.

(A) Wild-type inflorescence showing GUS activity in the axil and in the distal part of the pedicels.
(B) *bp* inflorescence showing GUS activity in the pedicels.
(C) *pny* inflorescence showing GUS activity in the pedicels.
(D) *bp pny* inflorescence showing GUS activity in the pedicels.
(E) Median longitudinal section through a wild-type stage 12 flower showing GUS activity restricted to the boundaries between floral organs (bar = 40 μm).
(F) Median longitudinal section through a *bp* stage 12 flower showing GUS activity in the pedicel (bar = 40 μm).
(G) Median longitudinal section through a *pny* stage 12 flower showing GUS activity in the pedicel (bar = 40 μm).
(H) Median longitudinal section through a *bp pny* stage 12 flower showing GUS activity in the pedicel (bar = 40 μm).
(I) Wild-type carpel showing GUS activity in boundaries between the valves and the replum.
(J) *bp* carpel showing GUS activity in valves margins.
(K) *pny* carpel showing GUS activity between the valves. The *pny* carpel has a narrower replum.
(L) *bp pny* carpel showing GUS activity between the valves.
(M) Longitudinal median section through a wild-type inflorescence meristem showing no GUS activity (bar = 40 μm).
(N) *bp* inflorescence meristem with no GUS activity (bar = 40 μm).
(O) Longitudinal section through a *pny* inflorescence meristem. GUS activity barely was detected (bar = 40 μm).
(P) *bp pny* inflorescence meristem with no GUS activity (bar = 40 μm).

than in the inflorescence meristem and results from growth variation (Peaucelle et al., 2007). No differences in the phyllotactic pattern could be detected in the *knat6* single mutant since 84% of the divergence angles fell into the 90° to 179° classes (Figure 7B). By contrast, a uniform distribution of divergence angles was observed in *pny*, confirming the disruption of the phyllotactic pattern in this mutant (Figure 7C). This defect was rescued in *knat6 pny* double mutants as 81% of the divergence angles fell into the 90° to 179° classes (Figure 7D). Together with the measurements of internode lengths between flowers, these

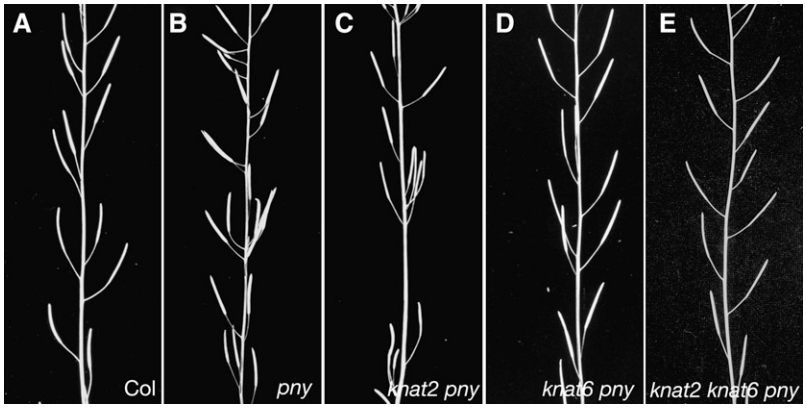

Figure 5. Phenotypes of the *knat2 pny*, *knat6 pny*, and *knat2 knat6 pny* Mutants.

(A) Wild-type inflorescence.
(B) *pny* inflorescence with irregular internode lengths.
(C) *knat2 pny* inflorescence. The inactivation of *KNAT2* did not alter the *pny* phenotype.
(D) *knat6 pny* inflorescence. The inactivation of *KNAT6* rescued the *pny* phenotype.
(E) *knat2 knat6 pny* inflorescence. The inactivation of *KNAT2* did not alter *knat6 pny* double mutant phenotype.

analyses indicate that the inactivation of *KNAT6* rescued the phyllotaxy defects of *pny*.

The *pny* mutant also exhibits defects in fruit development as the *pny* fruit shows a narrower replum, an abnormal pattern of lignification, and septum fusion defects (Roeder et al., 2003; Figures 8D to 8F compared with 8A to 8C). The replum and the septum of the *knat6* mutant were wild type (Figures 8G to 8I). Characterization of the *knat6 pny* fruit showed that the fruit defects seen in *pny* were rescued (Figures 8J to 8L). The *knat6 knat2 pny* triple mutant exhibited a wild-type phenotype (Figures 5 and 6; see Supplemental Figure 3 online). All together, these results show that the inactivation of *KNAT6* rescued the *pny* defects, whereas the inactivation of *KNAT2* did not have such an effect.

KNAT6 and *KNAT2* Expression Domains Are Enlarged in the *pny* Mutant

We then examined the expression patterns of *KNAT6* and *KNAT2* in the *pny* mutants using *PKNAT6-GUS* and *PKNAT2:GUS*, respectively. As shown in Figures 3C, 3G, 4C, and 4G, domains of both *KNAT6* and *KNAT2* expression were enlarged in *pny* pedicels. In wild-type plants, *KNAT2* and *KNAT6* are expressed in the SAM (Pautot et al., 2001; Belles-Boix et al., 2006) and are downregulated during floral transition. Figures 3M and 4M show that KNAT6-GUS and KNAT2-GUS activities were not detected in wild-type inflorescence meristems. In *pny* inflorescence meristems, KNAT6-GUS activity was not detected, whereas a weak KNAT2-GUS activity was detected (Figures 3O and 4O). Thus, the downregulation of *KNAT6* in the *pny* inflorescence meristem still was maintained, suggesting that the phyllotaxy defects seen in *pny* mutant results from the ectopic expression of *KNAT6* in the pedicels. By contrast, the altered expression of *KNAT2* observed in the *pny* mutant has no effect, as the *knat2 pny* double mutant exhibited a *pny* phenotype. Since the inactivation of *KNAT6* rescued the replum and septum *pny* defects, we also examined the expression pattern of *KNAT6* in *pny* carpels. The *KNAT2* expression was analyzed in parallel. In wild-type carpels, *KNAT2* and *KNAT6* expressions were restricted to the boundaries between the replum and ovary valves (Figures 3I and 4I; see Supplemental Figures 4C and 4D online; Pautot et al., 2001). In *pny* siliques, *KNAT6* and *KNAT2* expression domains coalesced due to the absence of the replum (Figures 3K and 4K).

The Inactivation of *KNAT6* Rescues Partially the *bp pny* Double Mutant Phenotype

To further examine the interaction with *BP* and *PNY*, we constructed the *knat6 bp pny* triple mutant. In parallel, we generated the *knat2 bp pny* and the *knat2 knat6 bp pny* mutants to test a potential redundancy of *KNAT6* with *KNAT2*. The *bp pny* double mutant shows an additive phenotype, with extremely short internodes, downward-oriented organ clusters, increased branching, and more severe fruit defects (Figures 9A and 10; Byrne et al., 2003; Smith and Hake, 2003; Alonso-Cantabrana et al., 2007). The inactivation of *KNAT2* and *KNAT6* in the *bp pny* background had distinct effects. While the *bp pny* alterations were attenuated in the absence of *KNAT2*, they were greatly reduced in the absence of *KNAT6* (Figures 9B, 9C, and 10). The average height of the *bp pny* mutant was 11.6 cm, whereas the average height of the wild type was 48.3 cm. The average heights of *knat2 bp pny* and *knat6 bp pny* were 20.7 and 39.8, respectively (Figure 10A). The *bp pny* mutant plants exhibited a strong loss of apical dominance as they produced 13 to 19 paraclades, whereas wild-type plants produced four to five paraclades (Figure 10B). This defect was partially rescued in the absence of *KNAT2* as *knat2 bp pny* produced 10 to 13 paraclades and almost restored in the absence of *KNAT6* as *knat6 bp pny* produced four to six paraclades (Figure 10B). One of the most striking features of the *bp pny* phenotype is the presence of extremely short internodes, with 88% of internodes ranging in length from 0 to 5 mm. This feature was slightly reversed in the absence of *KNAT2*, as

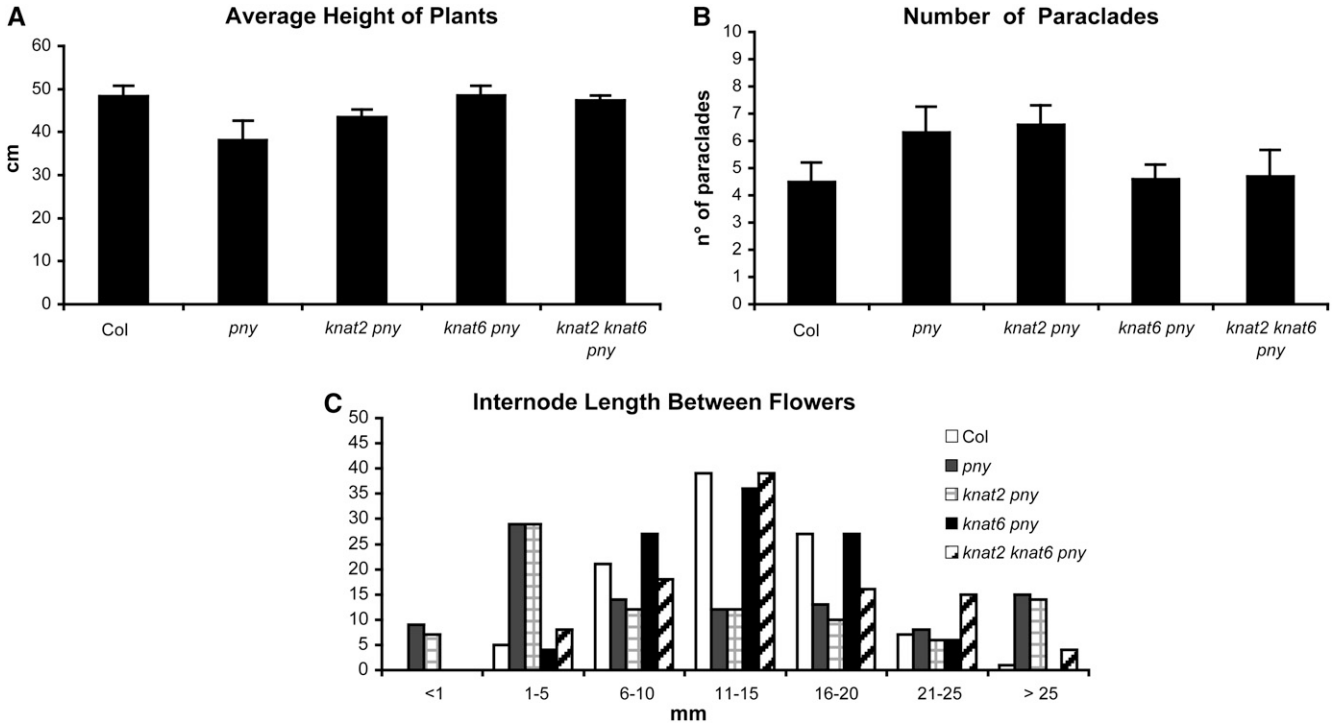

Figure 6. Quantitative Phenotypic Analyses of the *knat2 pny*, *knat6 pny*, and *knat2 knat6 pny* Mutants.

Ten plants for each genotype were analyzed.

(A) Average (+SD) height of wild-type, *pny*, *knat2 pny*, *knat6 pny*, and *knat2 knat6 pny* plants. The inactivation of *KNAT6* rescued the size defect of *pny*.

(B) Average (+SD) number of rosette paraclades of wild-type, *pny*, *knat2 pny*, *knat6 pny*, and *knat2 knat6 pny* plants. The partial loss of apical dominance of *pny* was rescued in the absence of *KNAT6*.

(C) Distribution of the length of the internode between two successive siliques. Ten internodes between the 1st and 11th siliques (counting acropetally) were measured. The distribution of siliques was wild type in *knat6 pny* and in *knat2 knat6 pny* mutants.

68% of the internodes ranged in length from 0 to 5 mm, and reversed to a greater extent in the absence of *KNAT6*, as 53% of the *knat6 bp pny* internodes were 6 to 15 mm long (Figure 10C). The *knat2 knat6 bp pny* quadruple mutant displayed the same phenotypic features as the *knat6 bp pny* triple mutant except for the orientation of the siliques. The average size of the quadruple mutant was 36.7 cm, with 50% of its internodes ranging in length from 6 to 15 mm, and the number of paraclades did not exceed 6 (Figure 10). The silique orientation defect was partially rescued in the absence of *KNAT6* and was suppressed in the absence of both *KNAT2* and *KNAT6* (Figure 10D). Thus, the defects seen in the *bp pny* double mutant were reduced greatly in the absence of *KNAT6*, confirming the higher impact of the *KNAT6* inactivation compared with *KNAT2*. Nevertheless, we found a slight effect of the *KNAT2* inactivation in the absence of both *BP* and *PNY*. The *KNAT2* effect on the orientation of the siliques was seen only when both *KNAT6* and *BP* were absent, as previously seen in the *knat2 knat6 bp* triple mutant.

We also checked whether *KNAT6* inactivation restored the replum defect seen in *bp pny. BP* is expressed in the replum, and a role for *BP* in replum development has been suggested recently (Alonso-Cantabrana et al., 2007). The *bp* mutant shows wild-type replum phenotypes, but its inactivation enhances the replum defect of *rpl* mutant alleles (Alonso-Cantabrana et al., 2007). By contrast, we showed that the inactivation of *KNAT6* rescued the *bp pny* replum defect (see Supplemental Figures 3I and 3K online). Thus, the inactivation of *KNAT6* had the opposite effect when compared with that of *BP* on replum development. This was consistent with the expression pattern of *KNAT6* that marked the boundaries between the replum and the valves (see Supplemental Figure 4D online). On the other hand, *KNAT2* expression overlaps with that of *KNAT6* in the carpel, but the inactivation of *KNAT2* did not have such an effect (Figures 3I and 4I; see Supplemental Figures 3G, 4C, and 4D online; Alonso-Cantabrana et al., 2007). *knat2 bp*, *knat6 bp*, and *knat2 knat6 bp* showed wild-type replum phenotypes, confirming that *KNAT6* and *KNAT2* are not redundant with *BP* for replum specification (see Supplemental Figures 3D to 3F online). By contrast, both *STM* and *BP* are expressed in the replum (see Supplemental Figures 4A and 4B online; Long et al., 1996; Alonso-Cantabrana et al., 2007). Together, this suggests that *STM* plays a redundant role with *BP* in replum specification and that *KNAT* class I members play distinct roles during carpel development.

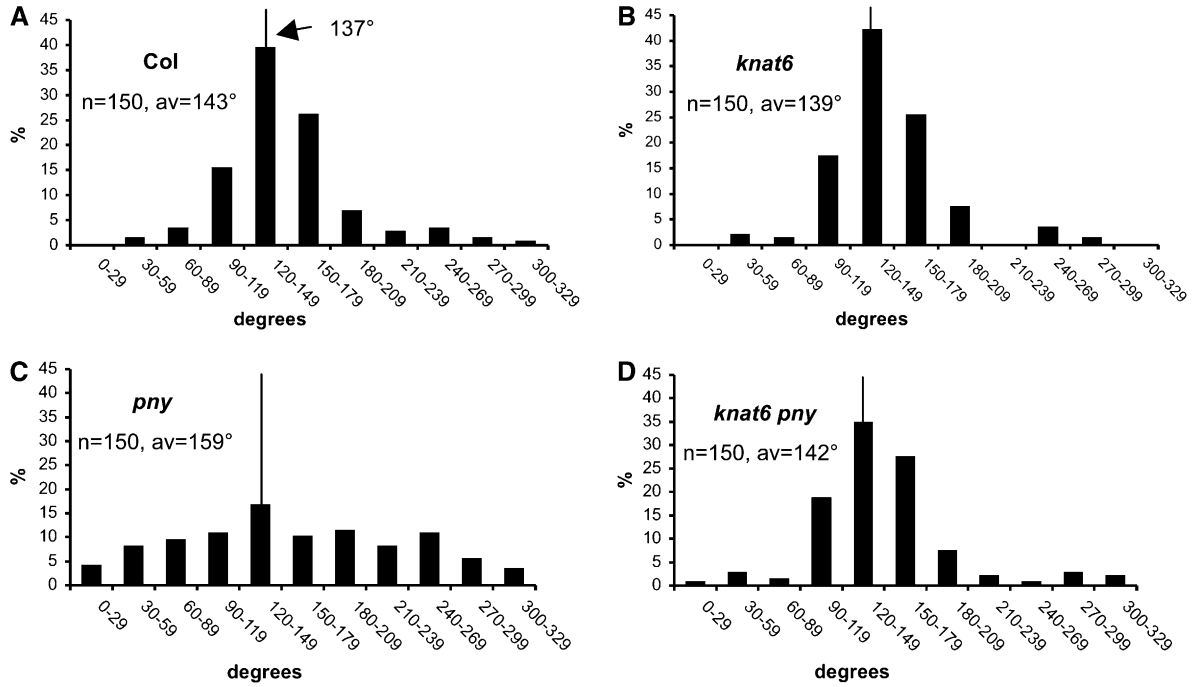

Figure 7. Phyllotaxy Measurements.

The divergence angle between two successives siliques along the main inflorescence was determined. Fifteen angles between the 1st and 16th siliques counting acropetally were measured. Ten plants for each genotype were analyzed. On each panel, the average value (av) is labeled, and the class containing the theoretical value (137°) is marked with a line.

(A) The distribution of divergence angles in the wild-type ecotype is shown.

(B) The *knat6* mutant phyllotactic pattern showed a wild-type distribution.

(C) The *pny* mutant had a uniform distribution of divergence angles.

(D) The *knat6 pny* double mutant phyllotactic pattern showed a wild-type distribution.

KNAT6 and *KNAT2* Expression Domains Are Enlarged in the *bp pny* Mutant

The expressions of *KNAT6* and *KNAT2* were examined in parallel in the *bp pny* double mutant. KNAT6-GUS activity was detected in the stems and pedicels of the *bp pny* double mutant (Figures 3D and 3H) and was not detected in *bp* and *bp pny* inflorescence meristems (Figures 3N and 3P). KNAT2-GUS activity was present in pedicels and barely was detected in inflorescence meristems of *bp pny* double mutants and was absent from *bp* inflorescence meristems (Figures 4D, 4H, 4N, and 4P). In *bp* carpels, KNAT6-GUS and KNAT2-GUS activities were restricted to the boundaries of the replum and ovary valves as in the wild type (Figures 3J and 4J). The expression domains of *KNAT6* and *KNAT2* in *bp pny* carpels coalesced as in *pny* (Figures 3L and 4L).

DISCUSSION

In this article, we examined the interaction of *KNAT6* and *KNAT2* with *BP* and *PNY* during inflorescence development. We previously showed that *KNAT6* contributes with *STM* to SAM function and boundary maintenance. *KNAT2* does not play such a role (Belles-Boix et al., 2006). Here, we showed that the loss of *KNAT6* partially rescues *bp* defects and suppresses *pny* alterations. The loss of *KNAT2* activity also partially rescues *bp* defects but only in the absence of *KNAT6* or in the absence of *PNY*.

BP and PNY Restrict *KNAT6* and *KNAT2* Expression to Promote Correct Inflorescence Development

Our genetic and expression analyses indicate that the defects seen in *pny*, and to a lesser extent in *bp*, are likely attributable to the misexpression of *KNAT6* since the removal of KNAT6 activity completely suppressed the *pny* defects and partially suppressed the *bp* defects. *KNAT2* also was misexpressed in *pny* and *bp*, but its inactivation had a weaker impact than that of *KNAT6*. In *bp* mutants, the effect of the *KNAT2* inactivation was restricted to the orientation of the siliques. Further experiments should be performed to determine whether BP and PNY directly interact with *KNAT6* and *KNAT2*. Motifs nearly identical to the BP/KNOX binding site were found in *KNAT2* and *KNAT6* genes (Mele et al., 2003). In wild-type plants, *BP* is expressed in the internodes and the pedicels and promotes their growth. The downward-pointing phenotype in *bp* is due to a defect in pedicel differentiation and fewer cell divisions (Venglat et al., 2002; Smith and Hake, 2003; Douglas and Riggs, 2005). Our data showed that this phenotypic feature was correlated with a misexpression of both *KNAT6* and

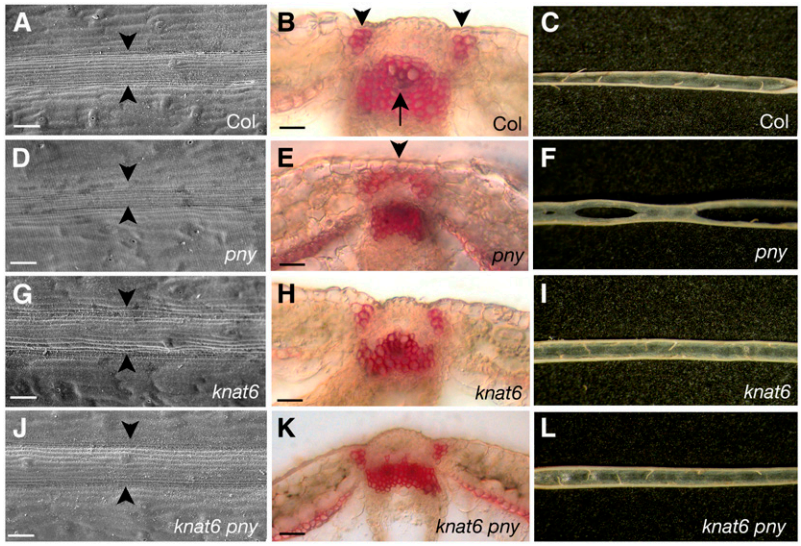

Figure 8. Phenotypes of the *pny*, *knat6*, and *knat6 pny* Siliques.

(A) to **(C)** Wild-type stage 17 fruit.
(A) Scanning electron micrograph showing the replum region (bar = 20 μm). The replum is the ridge between the two valves (arrowheads).
(B) Transverse section of the replum stained with phloroglucinol to detect lignification (pink). In the wild type, the lignification was detected at the valves margins (arrowheads) and in the inner replum (arrow) (bar = 40 μm).
(C) Septum.
(D) to **(F)** *pny* stage 17 fruit.
(D) Scanning electron micrograph showing a narrow replum region (arrowheads) (bar = 20 μm).
(E) Transverse section of *pny* fruit showing the lignified layer that extends across the replum.
(F) *pny* septum with fusion defects.
(G) to **(I)** *knat6* stage 17 fruit.
(G) Scanning electron micrograph showing a wild-type replum surface (bar = 20 μm).
(H) Transverse section of *knat6* fruit showing a wild-type lignification pattern (bar = 40 μm).
(I) The *knat6* septum was wild type.
(J) to **(L)** *knat6 pny* stage 17 fruit. The inactivation of *KNAT6* rescued *pny* fruit defects.
(J) Scanning electron micrograph showing a wild-type replum surface (bar = 20 μm).
(K) Transverse section of *knat6 pny* fruit showing a wild-type lignification pattern in the replum region (bar = 40 μm).
(L) The *knat6 pny* septum showing no fusion defects.

KNAT2. Consistent with these data, the inactivation of *KNAT6* and *KNAT2* restored the wild-type orientation of the pedicel. Given that the pedicel phenotype in *bp* is due to a shift toward differentiation, we found that KNAT class I proteins show distinct activities in the development of the pedicel, with *BP* counteracting the undifferentiated state maintained by *KNAT6* and *KNAT2*.

The interactions of *KNAT6* and *KNAT2* with *PNY* further confirmed their distinct activities: the inactivation of *KNAT6* suppressed the *pny* defects, while the inactivation of *KNAT2* did not. One of the most obvious defects of the *pny* mutant is its aberrant organ positioning. The *pny* mutants had internodes with irregular sizes and clusters of organs. In wild-type plants, organs are initiated successively on the flanks of the SAM with a spiral arrangement. This pattern, referred to as phyllotaxy, depends on predictive auxin gradients in the meristem (Reinhardt, 2005). However, previous studies indicated that the majority of *pny* mutants have a wild-type meristem structure. The size of the inflorescence meristem was slightly smaller and only 2 out 16 *pny* mutants showed an aberrant initiation of organs (Byrne et al., 2003). This suggests that the phyllotaxy defects seen in the *pny* mutant probably occurred during inflorescence growth. Our analyses indicated that the *knat6 pny* double mutant inflorescences had wild-type phyllotaxy. However, our expression analyses showed that the downregulation of *KNAT6* was maintained in *pny* inflorescence meristems. Therefore, the suppression of the aberrant organ positions in *knat6 pny* is likely attributable to the misexpression of *KNAT6* in *pny* pedicels, leading to abnormal pedicel differentiation. Our data are in agreement with recent data showing that phyllotaxy results not only from the pattern initiated in the meristem, but also from the subsequent growth during stem development. This was illustrated with plants disrupted in the microRNA regulation of the *CUP-SHAPED COTYLEDON2* (*CUC2*) gene: ectopic expression of *CUC2* in internodes leads to aberrant phyllotaxy (Peaucelle et al., 2007; Sieber et al., 2007). Both *CUC2* and *KNAT6* genes are expressed in restricted domains in wild-type meristems to specify boundaries. When they are ectopically expressed in the pedicel or in

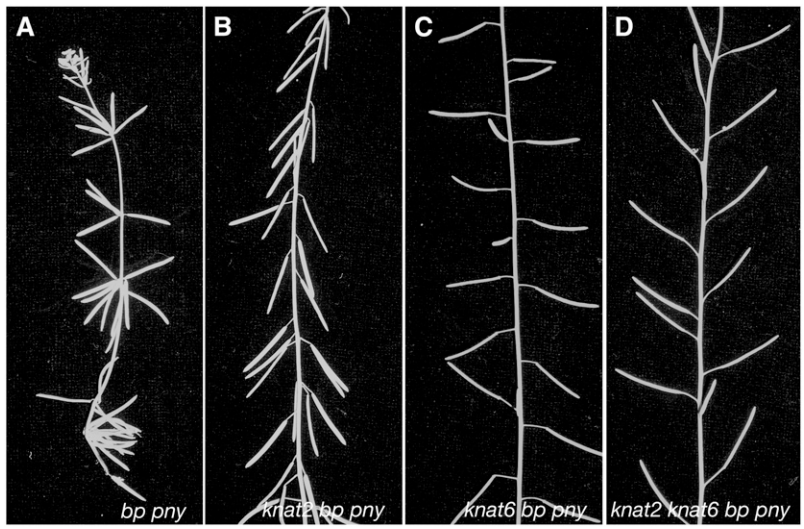

Figure 9. Phenotype of the *knat2 bp pny*, *knat6 bp pny*, and *knat2 knat6 bp pny* Mutants.

(A) *bp pny* inflorescence with clusters of downward-oriented organs.
(B) *knat2 bp pny* inflorescence. The inactivation of *KNAT2* partially rescued the *bp pny* phenotype.
(C) *knat6 bp pny* inflorescence. The inactivation of *KNAT6* partially rescued the *bp pny* phenotype.
(D) *knat2 knat6 bp pny* inflorescence showing a stronger restoration than the *knat2 bp pny* or *knat6 bp pny* inflorescences.

the internodes, they prevent the proper differentiation of those tissues. This indicates a similar effect of these two genes in and out of the SAM. Thus, our data suggest that in wild-type inflorescences, PNY restricts *KNAT6* expression to maintain the proper phyllotaxy during stem development. *KNAT2* also was misexpressed in *pny*, but its inactivation had no effect, suggesting a redundancy with other TALE members or a different role.

The interactions of *KNAT2* and *KNAT6* with *BP* and *PNY* confirmed the greater impact of *KNAT6* inactivation compared with *KNAT2* inactivation. This genetic analysis revealed an effect of *KNAT2* inactivation in the absence of both *PNY* and *BP*. This data confirms the redundancy between *KNAT2* and *KNAT6* in the absence of *BP*. Overlapping and distinct roles of transcription factors have been described for the homeodomain-leucine zipper family (Prigge et al., 2005). This type of interaction could provide flexibility in the regulation of distinct phases of development during plant growth.

The Loss of *KNAT6* Also Suppresses the *pny* Fruit Defect

In carpels, *KNAT6* and *KNAT2* are expressed in the boundaries between the replum and the valves, while *BP*, *STM*, and *PNY* are expressed in the replum (this work; Long et al., 1996; Roeder et al., 2003; Alonso-Cantabrana et al., 2007). Both its layered structure and its role in generating ovule primordia make the replum a true meristem. Recently, a role for *BP* in replum development has been suggested since the inactivation of *BP* enhances the replum defect of the *rpl* allele (Alonso-Cantabrana et al., 2007). By contrast, we showed that the inactivation of *KNAT6* suppresses the replum and septum defects seen in *pny* and in *bp pny*. Consistent with the absence of replum in *pny* siliques, *KNAT6* expression domains coalesced. This suggests that *PNY* restricts *KNAT6* in the wild type to promote replum identity. However, *PNY* is not required per se for replum specification, as double or triple mutant combinations involving *pny* or *rpl* alleles (*asymmetric leaves1 rpl*, *shatterproof1* [*shp1*] *shp2 rpl*, *jagged rpl*, *filamentous flower rpl*, and *knat6 pny*) develop a normal replum (this work; Roeder et al., 2003; Dinneny et al., 2005; Alonso-Cantabrana et al., 2007). This suggests that other factors are redundant to specify replum identity. Since the *knat2 knat6 bp* triple mutants had a normal replum, *STM* could play such a role. This is in agreement with the expression of *STM* in the replum.

METHODS

Plant Material and Growth Conditions

Arabidopsis thaliana plants were grown either on soil or in vitro as described by Hamant et al. (2002). All mutants used in this study are in the Col-0 background. Mutant alleles of *knat6-1*, *knat6-2*, and *knat2-5* were obtained from the Nottingham Arabidopsis Stock Centre (http://nasc.nott.ac.uk) and were previously described (Belles-Boix et al., 2006). The *bp-9* mutant allele was provided by Naomi Ori (Smith and Hake, 2003). The *pny* (*pny-40126* or *rpl-2*, Col background) mutant allele was obtained from the Nottingham Arabidopsis Stock Centre (http://nasc.nott.ac.uk) and described by Smith and Hake (2003). The translational *KNAT2-GUS* (Dockx et al., 1995) and transcriptional *KNAT6-GUS* (Belles-Boix et al., 2006) fusions have been described previously.

Plant Genetics

To construct the *knat6-1 pny* double mutant, plants homozygous for *knat6-1* were crossed to plants homozygous for *pny* (*pny*-40126), and *knat6-1 pny* double mutants were selected. Only two phenotypes segregated in the F2: the wild type and the *pny* phenotype. Genomic DNA

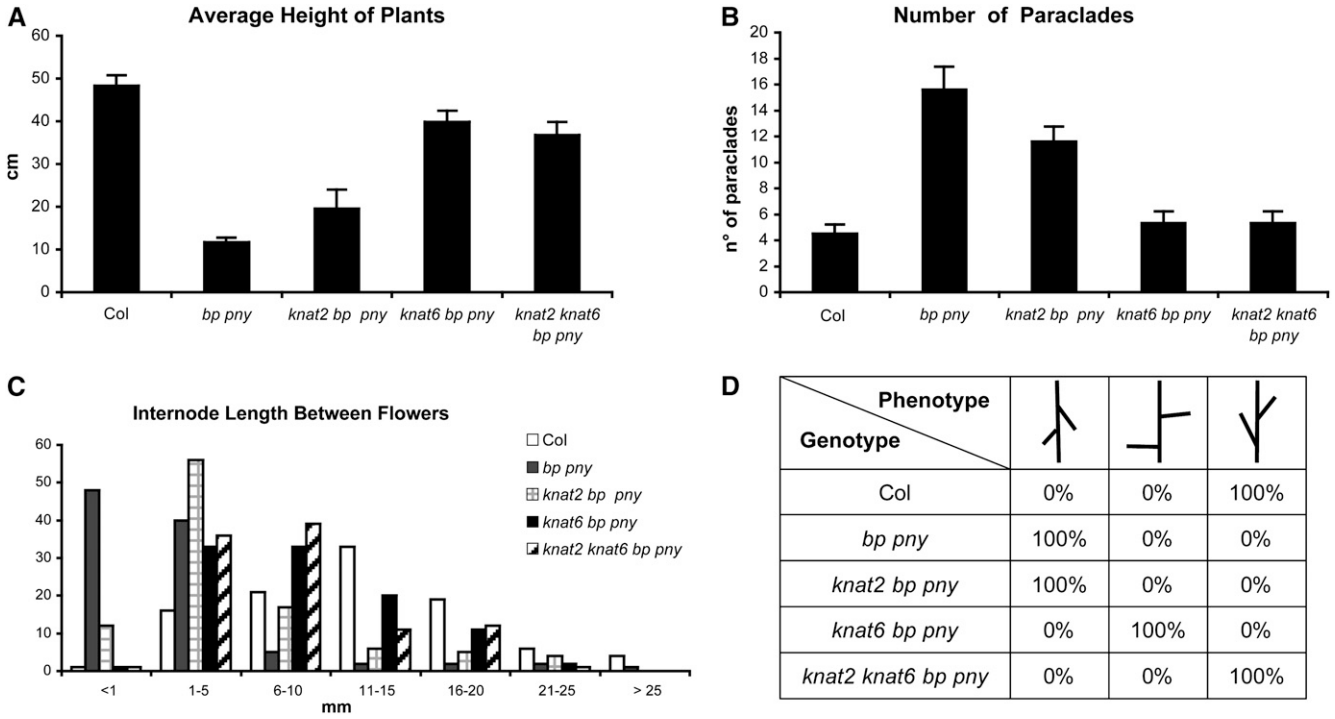

Figure 10. Quantitative Phenotypic Analyses of the *bp pny*, *knat2 bp pny*, *knat6 bp pny*, and *knat2 knat6 bp pny* Mutants.

Ten plants for each genotype were analyzed.

(A) Average (+SD) height of wild-type, *bp pny*, *knat2 bp pny*, *knat6 bp pny*, and *knat2 knat6 bp pny* plants. The shorter size of *bp pny* was partially rescued in the absence of *KNAT6* and to a lesser extent in the absence of *KNAT2*.

(B) Average (+SD) number of rosette paraclades of wild-type, *bp pny*, *knat2 bp pny*, *knat6 bp pny*, and *knat2 knat6 bp pny* plants. The *bp pny* partial loss of apical dominance was partially rescued in the absence of *KNAT6* and to a lesser extent in the absence of *KNAT2*.

(C) Distribution of the length of the internode between two successive siliques. Ten internodes between the 1st and 11th siliques (counting acropetally) were measured. The reduced size of internodes observed in *bp pny* was partially rescued in the absence of *KNAT6* and to a lesser extent in the absence of *KNAT2*.

(D) Orientation of the pedicels in the wild type, *bp pny*, *knat2 bp pny*, *knat6 bp pny*, and *knat2 knat6 bp pny*.

was extracted and analyzed by PCR to select *knat6-1 pny* double mutants. To detect the *knat6-1* allele, the T-DNA left border primer Lba 1 (5′-TGGTTCACGTAGTGGGCCATCG-3′) and the *KNAT6*-specific primer *KNAT6-03* (5′-GAAGATAAACCCTAGCTACAAG-3′) were used. The *KNAT6* wild-type allele was detected using the *KNAT6-03* and *KNAT6-04* (5′-AACCTGCATCGATCTATTTTC-3′) primers. The *pny-40126* allele was genotyped as described (Smith and Hake, 2003). The *knat6-1 pny* double mutant showed the wild-type phenotype. The same phenotype was observed when using the *knat6-2* allele. To detect the *knat6-2* allele, the T-DNA left border primer Lba 1 and the *KNAT6*-specific primer *KNAT6-15* (5′-AGATAAGTCGGTTCTGATGATG-3′) were used. The *KNAT6* wild-type allele was detected using *KNAT6-15* and *KNAT6-41* (5′-GCTACCAATCATTTTTCAGAAACTGGTCA-3′) primers.

To generate the *knat2-5 pny* double mutant, plants homozygous for *knat2-5* were crossed to plants homozygous for *pny* (pny-40126), and *knat2-5 pny* double mutants were selected. Only two phenotypes segregated in the F2: the wild type and the *pny* phenotype. Plants were analyzed by PCR to select the *knat2-5 pny* double mutant. To detect the *knat2-5* mutant allele, the T-DNA left border primer Lba 1 and the KNAT2-specific primer 4K1 (5′-CGCTTCTCATCCTTTGTATC-3′) were used. The *KNAT2* wild-type allele was detected using 4K1 and K11 (5′-TACCCAT-CAGTCTCTTAATG-3′) primers. The *knat2-5 pny* double mutant showed the *pny* phenotype.

To generate the *knat6-1 knat2-5 pny* triple mutant, plants homozygous for *knat6-1 pny* were crossed to plants homozygous for *knat2-5 pny*. Only two phenotypes segregated in the F2: the wild type and the *pny* phenotype. Plants were analyzed by PCR to select the *knat6-1 knat2-5 pny* triple mutant. The triple mutant exhibits the wild-type phenotype.

To generate the *knat6-1 bp-9* double mutant, plants homozygous for *knat6-1* were crossed to *bp-9*. Double mutants were selected by PCR analysis. To detect the *bp-9* mutant allele, the dSpm1 (5′- CTTATTT-CAGTAAGAGTGTGGGGTTTTGG-3′) and the *BP*-specific primer *BP-14* were used. The *BP* wild-type allele was detected with *BP-14* (5′-TGT-TAAGGGTTAGAACACCATG-3′) and *BP-3* (5′-GACAACAGCACCACTC-CTCAAA-3′) primers. The *bp* phenotype was partially rescued in the *knat6-1 bp-9* double mutant.

To generate the *knat2-5 bp-9* double mutant, plants homozygous for *knat2-5* were crossed to *bp-9*, and double mutants were selected by PCR analysis in the F2. The *knat2-5 bp-9* double mutant exhibits a *bp* phenotype.

To generate the *knat6-1 knat2-5 bp-9* triple mutant, plants homozygous for *knat6-1 bp-9* were crossed to plants homozygous for *knat2-5 bp-9*. Plants homozygous for *knat6-1 bp-9* and *knat2-5* were selected by PCR analysis. The *bp* phenotype was partially rescued in the *knat6-1 knat2-5 bp-9* triple mutant.

To generate the *bp-9 pny* double mutant, plants homozygous for *pny* were crossed to plants homozygous for *bp-9*. F2 plants showing the *bp-9 pny* phenotype were selected and checked by PCR analysis.

To generate the *knat6-1 bp-9 pny* triple mutant, the *knat6-1 pny* double mutant was crossed to the *knat6-1 bp*-9 double mutant. F2 plants homozygous for *knat6-1 bp-9 pny* were selected by PCR analysis. The *bp pny* phenotype was partially rescued in the *knat6-1 bp-9 pny* triple mutant.

To generate the *knat2-5 bp-9 pny* triple mutant, the *knat2-5 pny* double mutant was crossed to the *knat2-5 bp*-9 double mutant. F2 plants homozygous for *knat2-5 bp-9 pny* were selected by PCR analysis. The *knat2-5 bp pny* triple mutant showed a *bp pny* phenotype.

To generate the *knat6-1 knat2-5 bp-9 pny* quadruple mutant, the *knat6-1 bp-9 pny* triple mutant was crossed to the *knat2-5 bp*-9 *pny* triple mutant. F2 plants homozygous for *knat6-1 knat2-5 bp-9 pny* were selected by PCR analysis. The *bp pny* phenotype was partially rescued in the *knat6-1 knat2-5 bp-9 pny* quadruple mutant.

Phenotypic analyses were conducted on 10 plants for each genotype: *knat2-5*, *knat6-1*, *knat6-2*, *knat2-5 knat6-1*, *knat2-5 knat6-2*, *knat6-1 bp-9*, *knat2-5 bp-9*, *knat6-1 knat2-5 bp-9*, *knat6-1 pny*, *knat2-5 pny*, *knat6-2 pny, knat6-1 knat2-5 pny*, *knat2-5 bp-9 pny*, *knat6-1 bp-9 pny*, and *knat6-1 knat2-5 bp-9 pny.*

To examine the expression of *KNAT6* in *pny*, *bp*, and *bp pny*, the *PKNAT6-GUS* homozygous line was crossed to *pny*, *bp-9*, and the *bp-9 pny* double mutant. The F2 plants showing the *pny*, the *bp-9*, or the *bp-9 pny* phenotype, respectively, and KNAT6-GUS activity were selected. The F3 progenies of these F2 plants were examined for GUS activity to select plants homozygous for the *PKNAT6-GUS* construct.

To examine the expression of *KNAT2* in *pny*, *bp*, and *bp pny*, the *PKNAT2:GUS* homozygous line was crossed to the *pny*, the *bp-9*, or the *bp-9 pny* double mutant. F2 plants showing the *pny*, the *bp-9*, or the *bp-9 pny* phenotype, respectively, and KNAT2-GUS activity were selected. The F3 progenies of these F2 plants were examined for GUS activity to select plants homozygous for the *PKNAT2:GUS* construct.

Phenotypic Analysis

Quantitative analyses of the different genotypes were performed on 9-week-old plants as described (Smith and Hake, 2003). Ten plants for each genotype were used for phenotypic analyses. The phyllotaxy measurements were performed using the device described previously (Peaucelle et al., 2007). The divergence angle between the insertion points of two successive floral pedicels along the main inflorescence was measured. Fifteen divergence angles between the 1st and 16th siliques (counting acropetally) of each inflorescence were measured according to the orientation of the generative spiral.

In Situ Localization of GUS Activity

GUS staining was performed as described previously (Pautot et al., 2001). Tissue samples were fixed in 4% formaldehyde, dehydrated, and embedded in paraffin as described (Pautot et al., 2001). Paraffin sections (10 μm thick) were cut on a Leica-Jung (Leica Rueil-Malmaison) RM2055 rotary microtome carrying a disposable metal knife. Sections were attached to a precoated glass slide (Fisher) and photographed.

In Situ Hybridization

In situ hybridizations were performed as described previously (Belles-Boix et al., 2006). The *BP* antisense probe was generated using pDONOR201 that contains the *BP* cDNA as a template and using *BP-03* (5′-GACAACAGCACCACTCCTCAAA-3′) and *BP T7* (5′-TGTAATACGACTCACTATAGGGCTTATGGACCGAGACGATAAGG-3′), which incorporates a binding site for T7 polymerase, as primers. The *STM* antisense probe was generated using pDONOR201 that contains the *STM* cDNA as a template and using *STM-16* (5′-GGTTGTGGCGAGGCTAGAGG-3′) and *STM T7* (5′-TGTAATACGACTCACTATAGGGCTCAAAGCATGGTGGA-GGA-3′) as primers.

Lignin Staining

Carpels were embedded in 6% agarose (Sigma-Aldrich). Sections (70 μm thick) were cut on a Leica-VT 1000S (Leica Rueil-Malmaison) vibratome and stained with phloroglucinol (VWR Prolabo). Sections were photographed using a Nikon Microphot FXA microscope and a Jenoptik ProgRes C10 plus digital camera (Clara Vision).

Accession Numbers

Sequence data from this article can be found in the GenBank/EMBL data libraries under accession numbers At1g70510 (*KNAT2*), At1g23380 (*KNAT6*), At4g08150 (*BP*), At5g02030 (*PNY*), and At1g62360 (*STM).*

Supplemental Data

The following materials are available in the online version of this article.

Supplemental Figure 1. Phenotypes of the Wild Type *knat2-5*, *knat6-1*, *knat6-2*, *knat2-5 knat6-1*, and *knat2-5 knat6-2* Mutants.

Supplemental Figure 2. Quantitative Phenotypic Analyses of the *knat2-5*, *knat6-1*, *knat6-2*, *knat2-5 knat6-1*, and *knat2-5 knat6-2* Mutants.

Supplemental Figure 3. Lignin Pattern in *knat2*, *knat2 knat6*, *bp*, *knat2 bp*, *knat6 bp*, *knat2 knat6 bp*, *knat2 pny*, *knat2 knat6 pny*, *bp pny*, *knat2 bp pny*, *knat6 bp pny*, and *knat2 knat6 bp pny* Stage 17 Carpels.

Supplemental Figure 4. *KNAT* Class I Member Expression Domains Were Distinct in the Carpel.

ACKNOWLEDGMENTS

We thank the Salk Institute Genomic Analysis Laboratory for providing the sequence-indexed *Arabidopsis* T-DNA insertion mutants. We thank Naomi Ori for providing the *bp-9* mutant allele. We thank Bruno Letarnec for greenhouse management, Patrick Laufs for his hepful discussions, and Elisabeth Truernit and Olivier Hamant for critical reading of the manuscript. Enric Belles-Boix was funded by the Region Ile de France and the Institut National de la Recherche Agronomique. Laura Ragni and Markus Günl were supported by the European Marie-Curie (FP6) Program.

Received January 21, 2008; revised March 12, 2008; accepted March 17, 2008; published April 4, 2008.

REFERENCES

Alonso-Cantabrana, H., Ripoll, J.J., Ochando, I., Vera, A., Ferrandiz, C., and Martinez-Laborda, A. (2007). Common regulatory networks in leaf and fruit patterning revealed by mutations in the Arabidopsis ASYMMETRIC LEAVES1 gene. Development **134:** 2663–2671.

Belles-Boix, E., Hamant, O., Witiak, S.M., Morin, H., Traas, J., and Pautot, V. (2006). KNAT6: An Arabidopsis homeobox gene involved in meristem activity and organ separation. Plant Cell **18:** 1900–1907.

Bhatt, A.M., Etchells, J.P., Canales, C., Lagodienko, A., and Dickinson, H. (2004). VAAMANA – A BEL1-like homeodomain protein, interacts with KNOX proteins BP and STM and regulates inflorescence stem growth in Arabidopsis. Gene **328:** 103–111.

Byrne, M.E., Groover, A.T., Fontana, J.R., and Martienssen, R.A. (2003). Phyllotactic pattern and stem cell fate are determined by the Arabidopsis homeobox gene BELLRINGER. Development **130:** 3941–3950.

Byrne, M.E., Simorowski, J., and Martienssen, R.A. (2002). ASYMMETRIC LEAVES1 reveals knox gene redundancy in Arabidopsis. Development **129:** 1957–1965.

Clark, S.E., Jacobsen, S.E., Levin, J.Z., and Meyerowitz, E.M. (1996). The CLAVATA and SHOOT MERISTEMLESS loci competitively regulate meristem activity in Arabidopsis. Development **122:** 1567–1575.

Dinneny, J.R., Weigel, D., and Yanofsky, M.F. (2005). A genetic framework for fruit patterning in *Arabidopsis thaliana.* Development **132:** 4687–4696.

Dockx, J., Quaedvlieg, N., Keultjes, G., Kock, P., Weisbeek, P., and Smeekens, S. (1995). The homeobox gene ATK1 of *Arabidopsis thaliana* is expressed in the shoot apex of the seedling and in flowers and inflorescence stems of mature plants. Plant Mol. Biol. **28:** 723–737.

Douglas, S.J., Chuck, G., Dengler, R.E., Pelecanda, L., and Riggs, C.D. (2002). KNAT1 and ERECTA regulate inflorescence architecture in Arabidopsis. Plant Cell **14:** 547–558.

Douglas, S.J., and Riggs, C.D. (2005). Pedicel development in *Arabidopsis thaliana*: Contribution of vascular positioning and the role of the BREVIPEDICELLUS and ERECTA genes. Dev. Biol. **284:** 451–463.

Endrizzi, K., Moussian, B., Haecker, A., Levin, J.Z., and Laux, T. (1996). The SHOOT MERISTEMLESS gene is required for maintenance of undifferentiated cells in Arabidopsis shoot and floral meristems and acts at a different regulatory level than the meristem genes WUSCHEL and ZWILLE. Plant J. **10:** 967–979.

Hamant, O., Nogue, F., Belles-Boix, E., Jublot, D., Grandjean, O., Traas, J., and Pautot, V. (2002). The KNAT2 homeodomain protein interacts with ethylene and cytokinin signaling. Plant Physiol. **130:** 657–665.

Kanrar, S., Onguka, O., and Smith, H.M. (2006). Arabidopsis inflorescence architecture requires the activities of KNOX-BELL homeodomain heterodimers. Planta **224:** 1163–1173.

Long, J.A., Moan, E.I., Medford, J.I., and Barton, M.K. (1996). A member of the KNOTTED class of homeodomain proteins encoded by the STM gene of Arabidopsis. Nature **379:** 66–69.

Mele, G., Ori, N., Sato, Y., and Hake, S. (2003). The knotted1-like homeobox gene BREVIPEDICELLUS regulates cell differentiation by modulating metabolic pathways. Genes Dev. **17:** 2088–2093.

Pautot, V., Dockx, J., Hamant, O., Kronenberger, J., Grandjean, O., Jublot, D., and Traas, J. (2001). KNAT2: Evidence for a link between knotted-like genes and carpel development. Plant Cell **13:** 1719–1734.

Peaucelle, A., Morin, H., Traas, J., and Laufs, P. (2007). Plants expressing a miR164-resistant CUC2 gene reveal the importance of post-meristematic maintenance of phyllotaxy in Arabidopsis. Development **134:** 1045–1050.

Prigge, M.J., Otsuga, D., Alonso, J.M., Ecker, J.R., Drews, G.N., and Clark, S.E. (2005). Class III homeodomain-leucine zipper gene family members have overlapping, antagonistic, and distinct roles in Arabidopsis development. Plant Cell **17:** 61–76.

Ragni, L., Truernit, E., and Pautot, V. (2007). *KNOXing* on the *BELL:TALE* homeobox genes and meristem activity. Int. J. Plant Dev. Biol. **1:** 42–44.

Reinhardt, D. (2005). Regulation of phyllotaxis. Int. J. Dev. Biol. **49:** 539–546.

Roeder, A.H., Ferrandiz, C., and Yanofsky, M.F. (2003). The role of the REPLUMLESS homeodomain protein in patterning the Arabidopsis fruit. Curr. Biol. **13:** 1630–1635.

Sieber, P., Wellmer, F., Gheyselinck, J., Riechmann, J.L., and Meyerowitz, E.M. (2007). Redundancy and specialization among plant microRNAs: Role of the MIR164 family in developmental robustness. Development **134:** 1051–1060.

Smith, H.M., and Hake, S. (2003). The interaction of two homeobox genes, BREVIPEDICELLUS and PENNYWISE, regulates internode patterning in the Arabidopsis inflorescence. Plant Cell **15:** 1717–1727.

Venglat, S.P., Dumonceaux, T., Rozwadowski, K., Parnell, L., Babic, V., Keller, W., Martienssen, R., Selvaraj, G., and Datla, R. (2002). The homeobox gene BREVIPEDICELLUS is a key regulator of inflorescence architecture in Arabidopsis. Proc. Natl. Acad. Sci. USA **99:** 4730–4735.